NEUROSCIENCE

Synaptic mechanism underlying serotonin modulation of transition to cocaine addiction

Yue Li[1], Linda D. Simmler[1], Ruud Van Zessen[1], Jérôme Flakowski[1]†, Jin-Xia Wan[2,3], Fei Deng[2,3], Yu-Long Li[2,3], Katherine M. Nautiyal[4], Vincent Pascoli[1], Christian Lüscher[1,5]*

Compulsive drug use despite adverse consequences defines addiction. While mesolimbic dopamine signaling is sufficient to drive compulsion, psychostimulants such as cocaine also boost extracellular serotonin (5-HT) by inhibiting reuptake. We used SERT Met172 knockin (SertKI) mice carrying a transporter that no longer binds cocaine to abolish 5-HT transients during drug self-administration. SertKI mice showed an enhanced transition to compulsion. Conversely, pharmacologically elevating 5-HT reversed the inherently high rate of compulsion transition with optogenetic dopamine self-stimulation. The bidirectional effect on behavior is explained by presynaptic depression of orbitofrontal cortex–to–dorsal striatum synapses induced by 5-HT via 5-HT$_{1B}$ receptors. Consequently, in projection-specific 5-HT$_{1B}$ receptor knockout mice, the fraction of individuals compulsively self-administering cocaine was elevated.

With chronic consumption, ~20% of cocaine users lose control and are eventually diagnosed as addicted (*1*). An increase in dopamine (DA) levels is typical of all addictive drugs (*2*) and sufficient to trigger forms of synaptic plasticity underlying adaptive behaviors (*3*–*5*). This is exemplified by optogenetic DA neuron self-stimulation (oDASS), which induces neuronal adaptations similar to addictive drugs via selective release of DA from ventral tegmental area (VTA) neurons and yields a bimodal distribution of compulsive and noncompulsive individuals (*6*). Cocaine also inhibits the serotonin [5-hydroxytryptamine (5-HT)] transporter (SERT), causing 5-HT transients in the striatum. While pharmacological reduction of 5-HT in the entire forebrain can favor compulsive cocaine seeking (*7*) and differential efficacy of the 5-HT system may be involved in the vulnerability to drug addiction (*8*, *9*), the relevant circuits and underlying cellular mechanisms remain elusive. To parse the locus of 5-HT modulation, we took advantage of SERT Met172 knockin (SertKI) mice carrying a transporter that does not bind cocaine without altering the basal 5-HT levels (*10*–*12*). Genetically encoded 5-HT sensors (fig. S1) confirmed the absence of cocaine-evoked transients in the dorsal striatum (DS) of SertKIs [15 mg/kg ip (intraperitoneally)] (Fig. 1, A to C). Mice were trained to press a lever that triggered a cocaine intravenous infusion (0.5 mg/kg per infusion) accompanied by a cue light, followed by a progressive ratio (PR) session and four punishment (0.2-mA foot shock) sessions (Fig. 1D and fig. S2A). There was no difference between the SertKI and wild-type (WT) groups during the acquisition period (Fig. 1E). Facing punishment, however, some mice reduced cocaine self-administration (SA), while others continued unabated (Fig. 1F). An unbiased clustering analysis integrating four behavioral parameters over the last two punishment sessions yielded two clusters: renouncers and perseverers (Fig. 1, G and H). Out of 25 SertKI mice, 14 (56%) were classified as perseverers, in stark contrast to the 3 out of 26 (12%) in WT littermate mice (Fig. 1I). Perseverance was correlated neither to baseline cocaine SA (Fig. 1J) nor to the break point (fig. S2B), and the success rate accomplishing increasing break points did not differ between renouncers and perseverers of either genotype (Fig. 1K). Perseverers and renouncers across genotypes perceived pain similarly, as

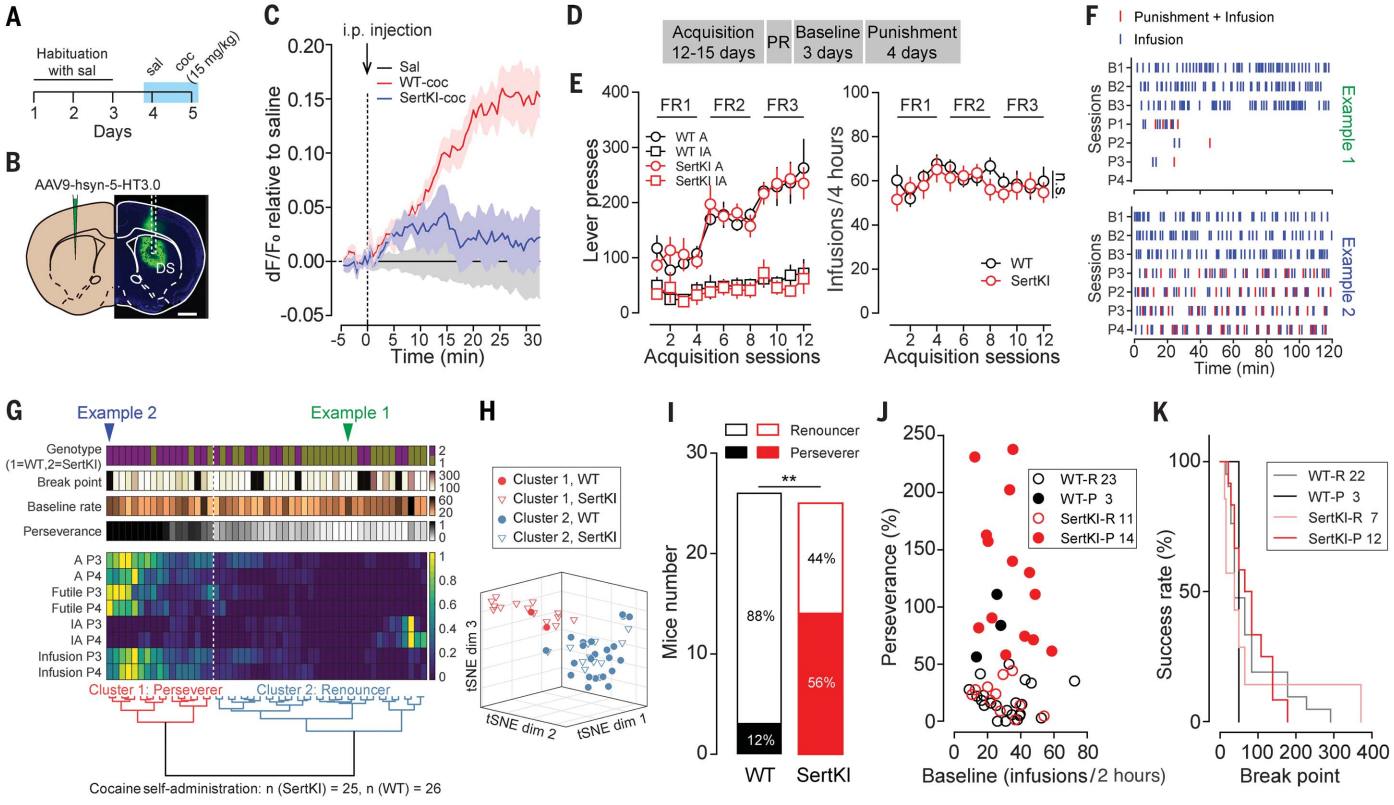

Fig. 1. SertKI animals are more compulsive for cocaine self-administration. (**A**) Schedule of saline and cocaine injections. (**B**) GRAB (G protein–coupled receptor activation–based) 5-HT sensor expression indicated with green fluorescent protein staining in the DS. Scale bar, 1 mm. (**C**) 5-HT transients in the DS induced by saline or cocaine (15 mg/kg) intraperitoneal injection in WT and SertKI mice (n = 3 mice for WT and SertKI group; data from saline-injected WT and SertKI are pooled). (**D**) Timeline of cocaine SA. (**E**) (Left) Number of active (A) and inactive (IA) lever presses of WT (black) and SertKI (red) animals (n = 26 and 25 mice for WT and SertKI groups, respectively) in acquisition sessions. (Right) Cocaine infusions obtained from WT (black) and SertKI (red) mice in acquisition sessions [two-way analysis of variance (ANOVA); $F_{1,588}$ = 1.996, P = 0.1583; n = 26 and 25 mice for WT and SertKI groups, respectively]. n.s., not significant. (**F**) Raster plots for infusions (blue lines) and punishments (red lines) in baseline and punishment sessions of a renouncer (WT mouse, top) and a perseverer (SertKI mouse, bottom). (**G**) Hierarchical clustering based on t-distributed stochastic neighbor embedding (tSNE) projection of different parameters of punishment sessions 3 and 4 (P3 and P4) of cocaine SA. Blue and green arrow heads indicate the examples presented in (F). (**H**) tSNE three-dimensional representation of clusters of perseverers (cluster 1) and renouncers (cluster 2) in cocaine SA. (**I**) Percentage of perseverers and renouncers among WT and SertKI groups (Fisher's exact test; $^{**}P$ = 0.001). (**J**) Perseverance rate as a function of the baseline rate (Pearson correlation coefficient r = −0.08; P = 0.55). (**K**) The success rate of performance as a function of the last progressive ratio value achieved by the mice (logrank test; P = 0.95). PR, progressive ratio; FR, fixed ratio; A, active lever presses; IA, inactive lever presses; R, renouncer; P, perseverer; sal, saline; coc, cocaine; WT, wild type; SertKI, SERT Met172 knockin. Data presented as means ± SEM.

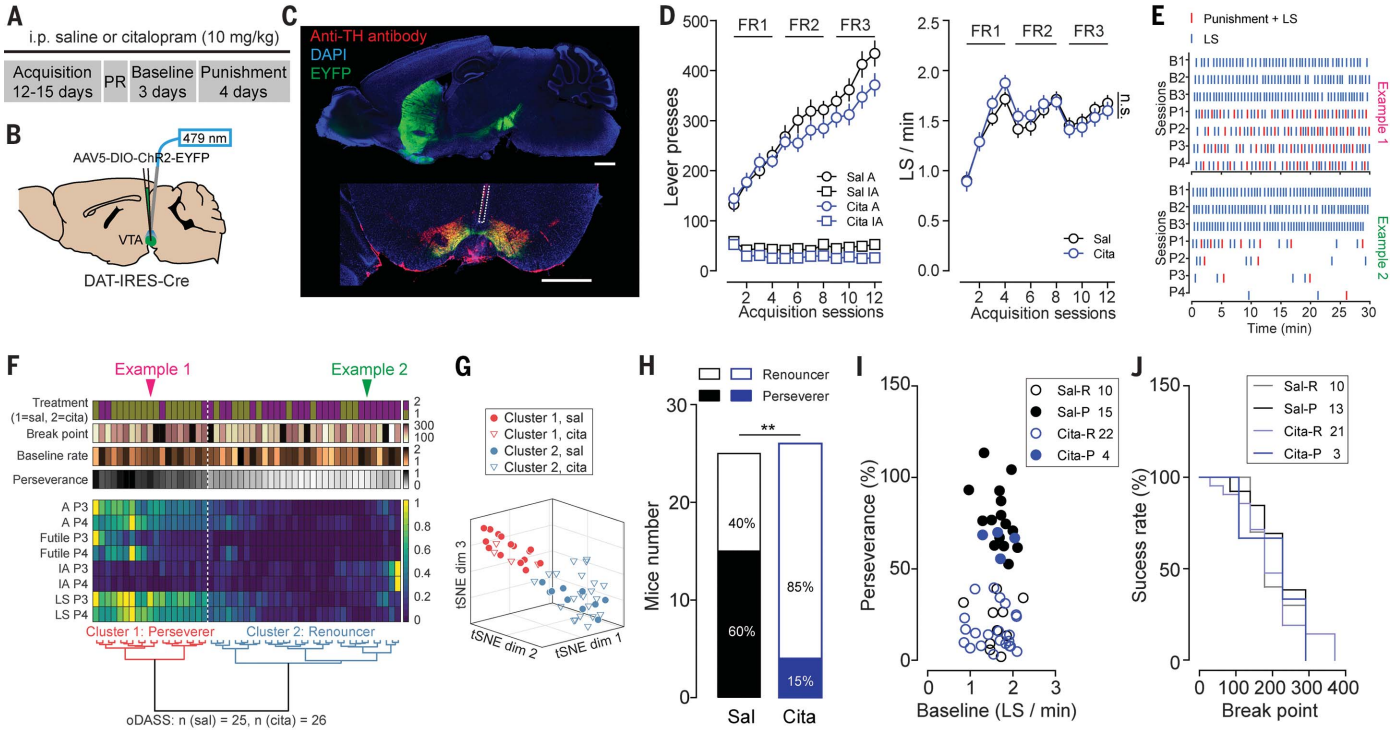

Fig. 2. Citalopram decreases compulsive dopamine self-stimulation. (**A**) Timeline of oDASS and saline or citalopram treatments. (**B**) Schematic of virus injection sites and optic fiber implantation sites. (**C**) ChR2-EYFP expression in the VTA from a sagittal slice (top image) and a coronal slice colabeled with tyrosine hydroxylase (TH; bottom image). Scale bars, 1 mm. (**D**) (Left) Number of active (A) and inactive (IA) lever presses of saline- (black) and citalopram-treated (blue) mice (n = 25 and 26 mice for saline and citalopram groups, respectively) in acquisition sessions. (Right) Laser stimulation per minute obtained from saline- (black) and citalopram-treated (blue) mice in acquisition sessions (two-way ANOVA; $F_{1,588}$ = 0.73, P = 0.39; n = 25 and 26 mice for saline and citalopram groups, respectively). (**E**) Raster plots for laser stimulations (blue lines) and punishments (red lines) in baseline and punishment sessions of a perseverer (top, from saline group) and a renouncer (bottom, from citalopram group). (**F**) Hierarchical clustering based on different parameters of punishment sessions 3 and 4 (P3 and P4) of oDASS. Red and green arrow heads indicate examples presented in (E). (**G**) tSNE three-dimensional representation of clusters of perseverers (cluster 1) and renouncers (cluster 2) in oDASS. (**H**) Percentage of perseverers and renouncers among saline- and citalopram-treated groups (Fisher's exact test; $^{**}P$ = 0.001). (**I**) Perseverance rate as a function of the baseline rate (Pearson r = 0.05; P = 0.71). (**J**) The success rate of performance as a function of the last progressive ratio value achieved by the mice (logrank test; P = 0.95). DAPI, 4′,6-diamidino-2-phenylindole; EYFP, enhanced yellow fluorescent protein; LS, laser stimulation; cita, citalopram. Data presented as means ± SEM.

[1]Department of Basic Neurosciences, Medical Faculty, University of Geneva, CH-1211 Geneva, Switzerland. [2]State Key Laboratory of Membrane Biology, Peking University School of Life Sciences, Beijing 100871, China. [3]IDG McGovern Institute for Brain Research, Peking University, Beijing 100871, China. [4]Department of Psychological and Brain Sciences, Dartmouth College, Hanover, NH 03755, USA. [5]Clinic of Neurology, Department of Clinical Neurosciences, Geneva University Hospital, CH-1211 Geneva, Switzerland.
***Corresponding author. Email: christian.luscher@unige.ch**
†Deceased.

hot plate latency was not affected by cocaine (fig. S2C).

Next, we did the converse. We gave mice access to oDASS, which leads to compulsion in more than half of individuals (*6*) and pharmacologically elevated 5-HT levels with citalopram (Fig. 2, A to C). Citalopram (10 mg/kg) induced robust 5-HT transients of a magnitude comparable to cocaine (fig. S1D). Active lever presses in mice that expressed ChR2 in VTA DA neurons induced a brief train of laser stimulations (LS; see methods in the supplementary materials). All mice readily mastered oDASS (Fig. 2D) regardless of pharmacological treatment, but major differences emerged when punishment was introduced (Fig. 2E). Clustering analysis, as described above, led to the emergence of perseverers and renouncers in both treatment groups (Fig. 2, F and G). However, only 4 out of 26 (15%) citalopram-treated mice were classified as perseverers, whereas in the saline-treated group, 60% were perseverers—a fraction similar to previous reports (*13*) (Fig. 2H). Again, the perseverance rate was uncorrelated to the baseline oDASS rate (Fig. 2I) or the break point (fig. S2D), and the success rate accomplishing each break point did not differ between renouncers and perseverers across treatment groups (Fig. 2J). For all groups and conditions, pain perception was similar (fig. S2E).

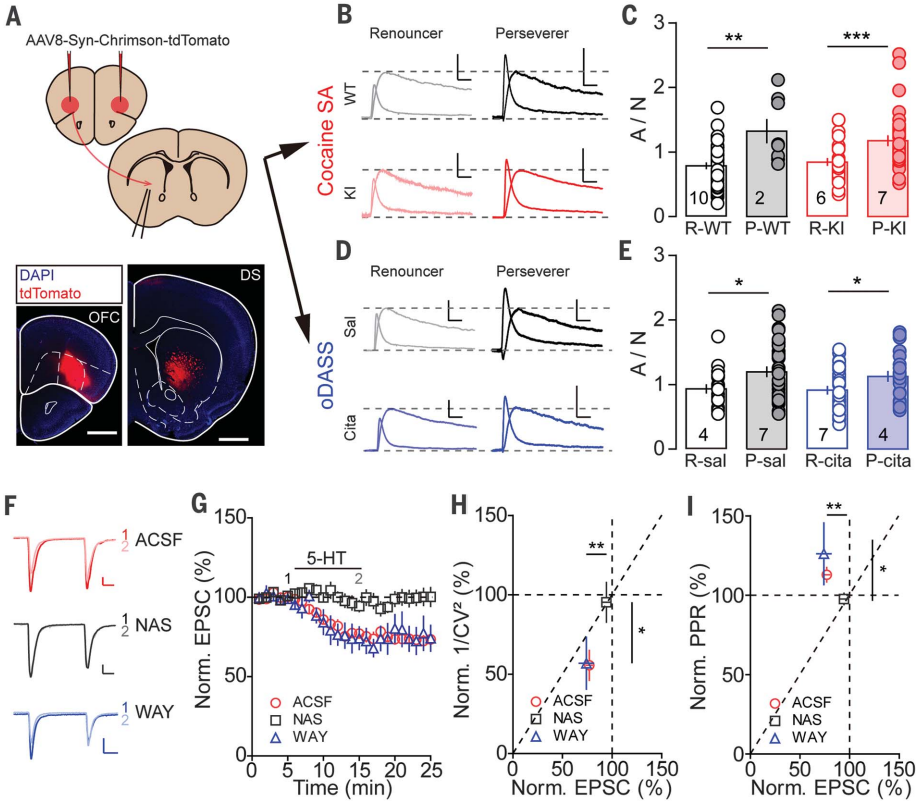

Fig. 3. The OFC-DS pathway is modulated by 5-HT. (**A**) (Top) Schematic of virus injection and recording sites. (Bottom) Chrimson-tdTomato–expressing cell bodies in the OFC (left) and terminals in the DS (right). Scale bars, 1 mm. (**B**) AMPA and NMDA currents at +40 mV of a renouncer (left) and a perseverer (right) from WT (upper) and SertKI (lower) group after cocaine SA. Scale bars, 200 pA, 15 ms. (**C**) Average AMPA/NMDA (A/N) of WT and KI renouncers and perseverers after cocaine SA (Mann Whitney test; $U = 74$, $^{**}P = 0.003$; $n = 53$ and 8 cells from ten and two mice for renouncer and perseverer in the WT group; $U = 252$, $^{***}P = 0.0001$; $n = 32$ and 35 cells from six and seven mice for renouncer and perseverer in SertKI group, respectively). (**D**) AMPA and NMDA currents at +40 mV of a renouncer (left) and a perseverer (right) from saline (upper) and citalopram (lower) treated group after oDASS. Scale bars, 200 pA, 15 ms. (**E**) Average A/N of saline- and citalopram-treated renouncers and perseverers after oDASS (two-tailed t test; $t_{54} = 2.54$, $^{*}P = 0.01$; $n = 21$ and 35 cells from four and seven mice for renouncer and perseverer in the saline-treated group, respectively; $t_{55} = 2.38$, $^{*}P = 0.02$; $n = 34$ and 23 cells from seven and four mice for renouncer and perseverer in the citalopram-treated group, respectively). (**F**) Traces before and after bath application of 5-HT in the presence of artificial cerebrospinal fluid (ACSF; red), NAS181 (gray), and WAY100635 (blue). Scale bars, 200 pA, 10 ms. (**G**) Average traces of EPSC before, during and after bath application of 5-HT in the presence of ACSF (red), NAS181 (gray), and WAY100635 (blue) ($n = 13$ and 14 cells from three mice for the ACSF and NAS181 groups, respectively, and seven cells from four mice for the WAY100635 group). (**H**) Normalized coefficient of variation ($1/CV^2$) versus normalized EPSC (one-way ANOVA; $F_{2,31} = 3.682$, $^{*}P = 0.0367$ for Norm. $1/CV^2$; $F_{2,31} = 7.948$, $^{**}P = 0.0016$ for Norm. EPSC; $n = 13$ and 14 cells from three mice for the ACSF and NAS181 groups, respectively, and seven cells from four mice for the WAY100636 group). (**I**) Normalized pair pulse ratio (PPR) versus normalized EPSC (Kruskal-Wallis test; $^{*}P = 0.041$ for Norm. PPR; $n = 13$ cells from three mice for the ACSF group, 10 and 6 cells from two mice for the NAS181 and WAY100636 groups, respectively). Data presented as means ± SEM.

Given that, for oDASS, the synaptic potentiation of afferents from the orbitofrontal cortex (OFC) to the DS drives perseverance (*13*), we wondered whether this is also the case for cocaine SA. To selectively stimulate the OFC-DS projection, we expressed the red-shifted opsin Chrimson in OFC neurons (Fig. 3A) and evoked excitatory postsynaptic currents (EPSCs) by illuminating the terminals in brain slices of the DS 24 to 48 hours after the last punishment session. The AMPA/NMDA (*N*-methyl-D-aspartate) ratio was higher in perseverers than in renouncers of cocaine SA as well as oDASS, regardless of genotypes and treatment (Fig. 3, B to E), confirming that a potentiated OFC-DS pathway reflects perseverance both in oDASS and cocaine SA. In no condition were the EPSCs rectifying (fig. S3), suggesting a potentiation by an increase in the number of AMPA receptors without a change in subunit composition, akin to the expression mechanism observed in individuals with compulsive oDASS (*13*).

We next examined the effect of 5-HT on synaptic transmission at the OFC-DS pathway in naïve mice. Bath application of 5-HT (4 μM) induced a presynaptic depression of excitatory transmission (Fig. 3, F and G), which could be blocked by 5-HT_{1B} receptor antagonist NAS181 (20 μM) but not by 5-HT_{1A} receptor antagonist WAY100*635* (1 μM) (Fig. 3, F and G). In line with the Gi/Go coupling of presynaptically located 5-HT_{1B} receptors, we observed a decreased coefficient variance ($1/CV^2$) and an increased paired pulse ratio (PPR), suggesting that the presynaptic depression was expressed by a reduction of glutamate release probability (Fig. 3, H and I). For confirmation, we evoked quantal events (qEPSCs) after replacing extracellular calcium (Ca^{2+}) with strontium (Sr^{2+}), thus desynchronizing light-evoked transmitter release (*14*), and found that the qEPSC frequency decreased

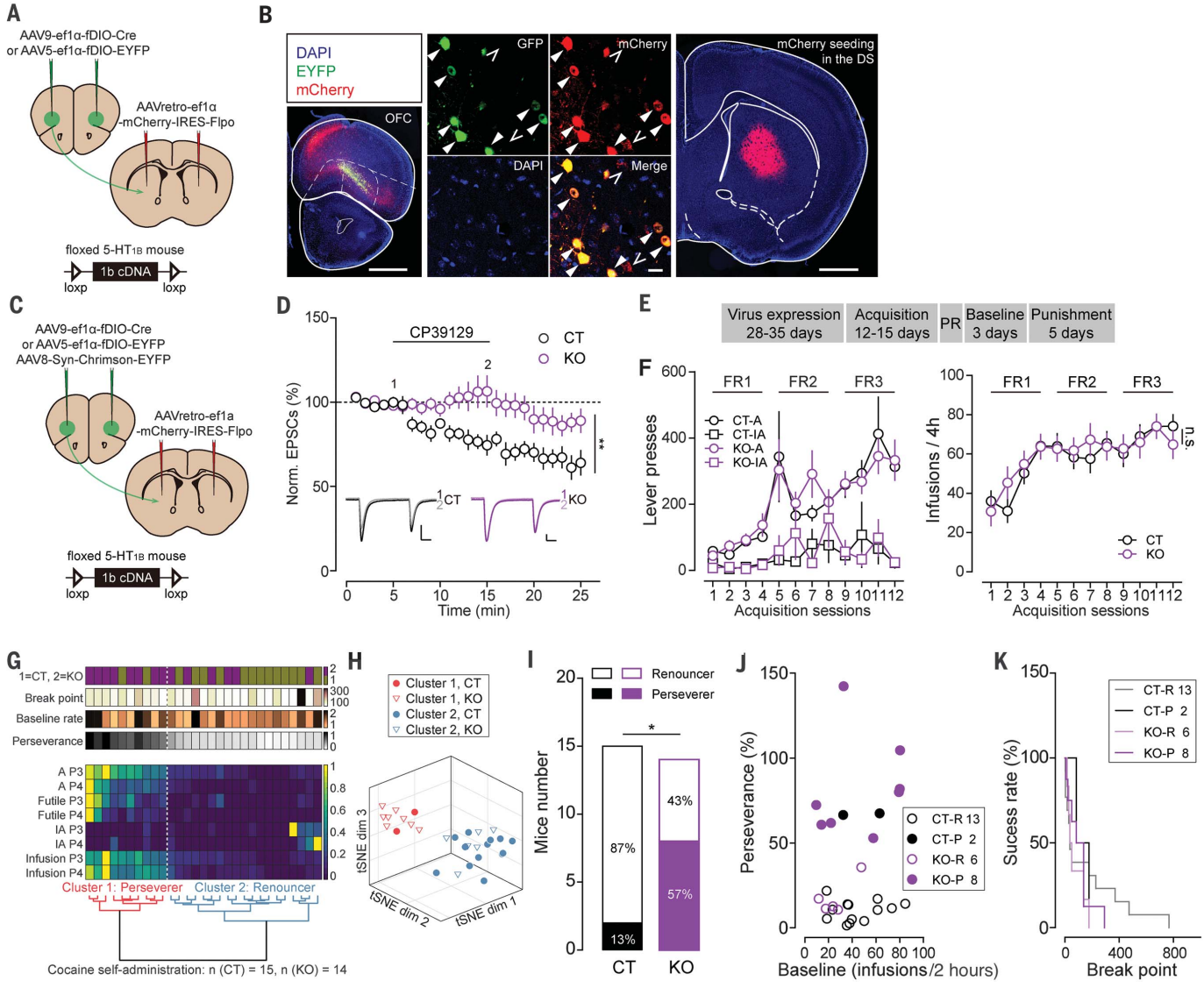

Fig. 4. Knocking out 5-HT$_{1B}$ receptors promotes compulsive cocaine self-administration. (**A**) Schematic of virus injections for cocaine SA. (**B**) (Left and middle) EYFP coexpressing with mCherry in the OFC. (Right) mCherry seeding in the DS. Scale bars, 1 mm (left and right) and 20 μm (middle). Arrows indicate DS projectors in the OFC expressing both EYFP and mCherry, open arrows indicate DS projectors expressing mCherry not infected by AAV-fDIO-EYFP. (**C**) Schematic of virus injections for patch clamp recording. (**D**) Average traces of EPSC before, during, and after bath application of 5-HT$_{1B}$ receptor agonist CP39129 in control (CT, black) and pathway-specific knockout 5-HT$_{1B}$ receptor (KO, violet) groups (compared Norm. EPSC recorded on last 5 min; two-tailed *t* test; t_{25} = 2.86, $^{**}P$ = 0.008; *n* = 15 and 12 cells from three mice for the CT and KO groups, respectively). Scale bars, 200 pA, 10 ms. (**E**) Timeline of virus injection and cocaine SA experiments. (**F**) (Left) Number of active (A) and inactive (IA) lever presses of CT (black) and KO (violet) mice in acquisition sessions. (Right) Cocaine infusions obtained by CT (black) and KO (violet) mice in acquisition sessions (two-way ANOVA; $F_{1,324}$ = 0.198, P = 0.66; *n* = 15 and 14 mice for the CT and KO groups, respectively). (**G**) Hierarchical clustering based on different parameters of punishment sessions 3 and 4 (P3 and P4) of cocaine SA. (**H**) tSNE three-dimensional representation of clusters of perseverers (cluster 1) and renouncers (cluster 2) in cocaine SA. (**I**) Percentage of perseverers and renouncers among CT and KO groups (Fisher's exact test; $^{*}P$ = 0.02). (**J**) Perseverance rate as a function of the baseline rate (Pearson r = 0.20; P = 0.30). (**K**) The success rate of performance as a function of the last progressive ratio value achieved by the mice (logrank test; P = 0.84). Data presented as means ± SEM.

but the amplitude stayed unchanged (fig. S4, A to C). Furthermore, 5-HT induced presynaptic depression in both D1-positive and D1-negative neurons obtained from D1-tdTomato mice (fig. S4D), consistent with previous reports (*15*, *16*).

We next hypothesized that presynaptic depression may reduce the likelihood for long-term potentiation (LTP) at the OFC- DS synapse, which in turn would prevent the transition to compulsion in cocaine SA. This seems plausible since chemogenetic reduction of OFC activity also reduced the fraction of perseverers in oDASS (*6*). Therefore, to establish a causal link between 5-HT–induced presynaptic depression and compulsive cocaine use, we aimed to abolish 5-HT$_{1B}$ receptors selectively in the OFC neurons targeting the DS. We injected

retroAAV-ef1α-mCherry-IRES-Flpo in the DS of 5-HT_{1B} floxed mice (*17*). This led to Flpo expression in OFC neurons targeting the DS. AAV9-ef1α-fDIO-Cre or control virus was then injected in the OFC to express Cre in OFC cells targeting the DS (Fig. 4, A and B), which then led to recombination and abolishment of 5-HT_{1B} receptors. We confirmed the successful receptor knockout functionally by the inability of 5-HT_{1B} agonist CP39129 (2 μM) to induce a presynaptic depression (Fig. 4, C and D).

A month after virus injection, the 5-HT_{1B} knockout mice learned to self-administer cocaine (Fig. 4E). We observed an acquisition period (Fig. 4F) similar to the one described above (Fig. 1E). Once punishment was introduced, we again observed persevering and renouncing mice (Fig. 4, G and H), with a higher fraction of perseverers in the projection-specific 5-HT_{1B} knockout compared to the control group (57% versus 13%) (Fig. 4I). Perseverance was unrelated to baseline performance (Fig. 4J), or break point in the two groups, in both control and knockout mice (Fig. 4K). The percentage of perseverers in the 5-HT_{1B} knockout group was very close to the fraction of perseverers in the SertKI group and in saline-treated oDASS mice.

A synaptic mechanism thus emerges that underlies a modulatory role of 5-HT reducing the likelihood of transition to compulsion and eventually addiction (see fig. S5). In WT mice, cocaine binds to SERT to block 5-HT reuptake. The elevated extracellular 5-HT activates 5-HT_{1B} receptors and causes presynaptic depression of OFC terminals. This reduces the likelihood of inducing postsynaptic potentiation at OFC-DS synapses that ultimately drives compulsion. In SertKI mice, cocaine cannot bind to SERT, and extracellular 5-HT remains unaffected by cocaine infusions (*10*). An OFC-DS transmission not undergoing presynaptic depression may thus enhance the likelihood of LTP induction, and the stochastic process would then show as a higher fraction of compulsive individuals. In 5-HT_{1B} knockout mice, although cocaine still inhibits 5-HT reuptake, the OFC-DS transmission is not depressed, which again may favor LTP induction. This interpretation is in line with the report that genome-wide 5-HT_{1B} receptor knockout mice are more impulsive (*17*). These mice are also more vulnerable to cocaine (*18*), which raises the possibility that individual addiction liability may be determined by 5-HT signaling. Variation in 5-HT synthesis, synaptic release, efficiency of reuptake, and extracellular levels could be additional determinants of overall vulnerability. Here we reveal addiction liability once 5-HT modulation has been eliminated, which is in line with the general idea that 5-HT opposes DA effects to inhibit behavior (*19*). However, this model is challenged by the observation that selective activation of 5-HT neurons allows high motivation to be maintained during complex tasks (*20*, *21*).

While our study focused on cocaine, 5-HT may also counteract the transition to compulsion when other addictive drugs are consumed (*8*, *9*). Amphetamine, despite having a relatively low SERT affinity, increases nonvesicular release of 5-HT, and opioids may indirectly activate 5-HT neurons in the dorsal raphe (*22*–*24*). In fact, the ratio between dopamine transporter and SERT affinity may predict the addiction liability of emerging drugs (*25*). This may also apply to natural rewards such as food and sex, but these have low addiction liabilities, making empirical testing a challenge. Finally, it may also be interesting to explore whether 5-HT modulation levels may not only prevent the transition to compulsion but also facilitate regaining control, as suggested by pharmacological interventions in rodents in a distinct behavioral paradigm. Forebrain 5-HT_{2C} receptors may inhibit compulsive cocaine seeking after compulsion is established (*7*), possibly via modulation of acute effects and early adaptive behaviors (*26*). By contrast, our data show that pathway-specific knockout of 5-HT_{1B} receptors does not affect acquisition or motivation for cocaine and specifically modulates compulsion. Three days of 5-HT_{1B} agonist (CGS12066B; 10 mg/kg, 30 min intraperitoneal injection before each session) treatment after the last punishment session of oDASS left perseverance to oDASS intact (fig. S6), suggesting that 5-HT_{1B} receptor activation prevents transition to compulsion but cannot reverse it once it is established.

The present mechanistic investigation may help to refine approaches to overcome the limitations and diverging findings on the efficacy of 5-HT reuptake blockers in pilot studies with human addicts (*27*–*29*) or to design selective agonists complementing the empirical use of hallucinogens in addiction treatments (*30*). In summary, 5-HT emerges as a modulator of the progression to compulsion via the convergence on key synaptic mechanisms in the framework of the current circuit model for addiction (*5*).

REFERENCES AND NOTES

1. M. Yücel *et al*., *Addiction* **114**, 1095–1109 (2019).
2. C. Lüscher, M. A. Ungless, *PLOS Med.* **3**, e437 (2006).
3. C. Lüscher, R. C. Malenka, *Neuron* **69**, 650–663 (2011).
4. C. Lüscher, *Annu. Rev. Neurosci.* **39**, 257–276 (2016).
5. C. Lüscher, P. H. Janak, *Annu. Rev. Neurosci.* **44**, 173–195 (2021).
6. V. Pascoli, J. Terrier, A. Hiver, C. Lüscher, *Neuron* **88**, 1054–1066 (2015).
7. Y. Pelloux, R. Dilleen, D. Economidou, D. Theobald, B. J. Everitt, *Neuropsychopharmacology* **37**, 2505–2514 (2012).
8. L. G. Kirby, F. D. Zeeb, C. A. Winstanley, *Neuropharmacology* **61**, 421–432 (2011).
9. C. P. Müller, J. R. Homberg, *Behav. Brain Res.* **277**, 146–192 (2015).
10. B. J. Thompson *et al*., *Proc. Natl. Acad. Sci. U.S.A.* **108**, 3785–3790 (2011).
11. L. D. Simmler, R. D. Blakely, *ACS Chem. Neurosci.* **10**, 3053–3060 (2019).
12. L. D. Simmler *et al*., *Br. J. Pharmacol.* **174**, 2716–2738 (2017).
13. V. Pascoli *et al*., *Nature* **564**, 366–371 (2018).
14. S. H. Oliet, R. C. Malenka, R. A. Nicoll, *Science* **271**, 1294–1297 (1996).
15. G. Dölen, A. Darvishzadeh, K. W. Huang, R. C. Malenka, *Nature* **501**, 179–184 (2013).
16. B. N. Mathur, N. A. Capik, V. A. Alvarez, D. M. Lovinger, *J. Neurosci.* **31**, 7402–7411 (2011).
17. K. M. Nautiyal *et al*., *Neuron* **86**, 813–826 (2015).
18. B. A. Rocha *et al*., *Nature* **393**, 175–178 (1998).
19. Y. L. Boureau, P. Dayan, *Neuropsychopharmacology* **36**, 74–97 (2011).
20. Z. Liu *et al*., *Neuron* **81**, 1360–1374 (2014).
21. E. Lottem *et al*., *Nat. Commun.* **9**, 1000 (2018).
22. P. Scholze *et al*., *J. Pharmacol. Exp. Ther.* **293**, 870–878 (2000).
23. L. D. Simmler *et al*., *Br. J. Pharmacol.* **168**, 458–470 (2013).
24. R. Tao, S. B. Auerbach, *J. Pharmacol. Exp. Ther.* **303**, 704–710 (2002).
25. M. Liechti, *Swiss Med. Wkly.* **145**, w14043 (2015).
26. P. J. Fletcher, A. J. Grottick, G. A. Higgins, *Neuropsychopharmacology* **27**, 576–586 (2002).
27. S. Vayalapalli, M. Vaughn, K. Salles-Shahid, J. Byrd-Sellers, K. Drexler, *Am. J. Addict.* **20**, 485–486 (2011).
28. F. G. Moeller *et al*., *Am. J. Drug Alcohol Abuse* **33**, 367–378 (2007).
29. J. Grabowski *et al*., *J. Clin. Psychopharmacol.* **15**, 163–174 (1995).
30. L. P. Cameron *et al*., *Nature* **589**, 474–479 (2021).
31. Y. Li *et al*., Synaptic mechanism underlying serotonin modulation of transition to cocaine addiction, Version 1, Zenodo (2021); https://doi.org/10.5281/zenodo.5091499.

ACKNOWLEDGMENTS

In memory of our dear colleague Jérôme Flakowski, who died on 11 May 2021. We thank R. D. Blakely from the Florida Atlantic University Brain Institute for providing SertKI mice. We thank all lab members for suggestions and comments on the experiments and manuscript. We also thank C. Bellone, B. Everitt, and F. Markopoulos for critical comments on the manuscript. **Funding:** This work was supported by the Swiss National Science Foundation and the European Research Council (C.L.) and R01 MH126178 (K.M.N.). **Author contributions:** Conceptualization: Y.L., V.P., and C.L. Investigation: Y.L., L.D.S., and V.P.; Data analysis: Y.L., R.V.Z., and J.F. Visualization: Y.L. and J.F. Reagents: K.M.N., J.-X.W., F.D., and Y.-L.L. Funding acquisition: C.L. Supervision: C.L. Writing: Y.L., V.P., and C.L. Senior authors: Y.-L.L., K.M.N., V.P., and C.L. **Competing interests:** The authors declare that they have no competing interests. **Data and materials availability:** All data, code, and materials are available on Zenodo (*31*).

SUPPLEMENTARY MATERIALS

https://science.org/doi/10.1126/science.abi9086
Materials and Methods
Figs. S1 to S6
References (*32*, *33*)
MDAR Reproducibility Checklist

View/request a protocol for this paper from *Bio-protocol*.

9 April 2021; accepted 20 July 2021
10.1126/science.abi9086

Science

Synaptic mechanism underlying serotonin modulation of transition to cocaine addiction

Yue LiLinda D. SimmlerRuud Van ZessenJérôme FlakowskiJin-Xia WanFei DengYu-Long LiKatherine M. NautiyalVincent PascoliChristian Lüscher

Science, 373 (6560), • DOI: 10.1126/science.abi9086

Prevention of compulsive cocaine taking

Over time, about 20% of chronic cocaine users lose control and become addicted. There are indications that the differential efficacy of the brain serotonin (5-HT) system may be involved in the vulnerability to drug addiction. However, the relevant circuits and underlying cellular processes remain elusive. Li *et al*. discovered a synaptic mechanism in mice that underlies the modulatory role of 5-HT in reducing the likelihood of transition to compulsion and eventually addiction (see the Perspective by Miyazaki and Miyazaki). Cocaine binds to 5-HT transporters to block 5-HT reuptake. The elevated extracellular 5-HT activates 5-HT receptors and causes presynaptic depression of a projection from the orbitofrontal cortex to the dorsal striatum. These changes reduce the likelihood of inducing postsynaptic potentiation at these synapses, which ultimately drives compulsion. —PRS

Science (ISSN) is published by the American Association for the Advancement of Science. 1200 New York Avenue NW, Washington, DC 20005. The title *Science* is a registered trademark of AAAS.